

Investigation of the unique nulling properties of PSR B0818–41

Bhaswati Bhattacharyya¹, Yashwant Gupta², Janusz Gil³

¹*Inter-University Centre for Astronomy and Astrophysics, Pune University Campus, Pune 411 007, India*

²*National Centre for Radio Astrophysics, TIFR, Pune University Campus, Post Bag 3, Pune 411 007, India*

³*Institute of Astronomy, University of Zielona Gora, Lubuska 2, 65-265 Zielona Gora, Poland*

Accepted. Received

ABSTRACT

We report on the unique nulling properties of PSR B0818–41, using the GMRT at 325 and 610 MHz. This pulsar shows well defined nulls, with lengths ranging from a few tens of pulses to a few hundreds of pulses. We estimate a nulling fraction of about 30% at 325 MHz. Furthermore, we find the following interesting behaviour of the pulse intensities, pulse shapes, pulse widths and the drift rate, just before and after the nulls: (i) There is a clear difference between the transitions from bursts to nulls to that from the nulls to bursts. The pulsar’s intensity does not switch off abruptly at the null, but fades gradually, taking $\sim 10P_1$. On the other hand, just after the nulls the intensity rises to a maximum over a short (less than one period) time scale. (ii) While the last active pulses before nulls are dimmer, the first few active pulses just after the nulls outshine the normal ones. This effect is very clear for the inner region of the pulsar profile, where the mean intensity of the last few active pulses just after the nulls is ~ 2.8 times more than that for the last active pulses just before the nulls. (iii) There is a significant evolution of the shape of the pulsar’s profile, around the nulls, especially at the beginning of the bursts: an enhanced bump of intensity in the inner region, a change in the ratio of the strengths of the leading and trailing peaks towards a more symmetric profile, an increase in profile width of about 10%, and a shift of the profile centre towards later longitudes. Some of these can be explained by a (temporary?) shift of the emission regions to different heights and/or slightly outer field lines in the magnetosphere. (iv) Just before the onset of the nulls, for about 60% of the occasions, the apparent drift rate becomes slower (correlated with the gradual decrease of pulse intensity), transitioning to an almost phase stationary drift pattern. Further, when the pulsar comes out of the null, the increased intensity is very often accompanied by what looks like a disturbed drift rate behaviour, which settles down to the regular drift pattern as the pulsar intensity returns to normal. Thus, we find some very specific and well correlated changes in the radio emission properties of PSR B0818–41 when the emission restarts after a null. These could imply that the phenomenon of nulling is associated with some kind of a “reset” of the pulsar radio emission engine. We also present plausible explanations for some of the observed behaviour, using the Partially Screened Gap model of the inner pulsar accelerator.

Key words: Stars: neutron – stars: pulsars: general – stars: pulsar: individual: **PSR B0818–41**

1 INTRODUCTION

Many pulsars are known to exhibit the phenomenon of nulling, where the emission appears to cease, or is greatly diminished, for a certain number of pulse periods. Nulling is considered an important clue towards unraveling the mystery of the pulsar emission mechanism. Detailed investigation of nulling for many pulsars in several works (e.g. Ritchings (1976), Rankin (1986), Biggs (1992)), has established that nulling is intrinsic to individual pulsars and possibly broadband in radio frequency. Though nulling is known to occur randomly, there are some recent studies by Rankin & Wright

(2008) and Herfindal & Rankin (2007) which report periodicity in nulling for quite a few pulsars. It is generally believed that onset of nulling is abrupt, i.e. pulse intensity drops suddenly at the onset of a null. However, for PSR B0809+74 and PSR B1944+17, it is reported that the transitions from bursts to nulls show a gradual decline of pulse energy, while transitions from nulls to bursts are abrupt (Lyne & Ashworth (1983), Deich et al. (1986)). On the other hand, for PSR B0031–07, the onset of nulls is found to be abrupt (Vivekanand 1995). Lyne & Ashworth (1983) investigated the pre and post null behavior of PSR B0809+74 and reported a relative dimness of the last few pulses before nulls, whereas the first

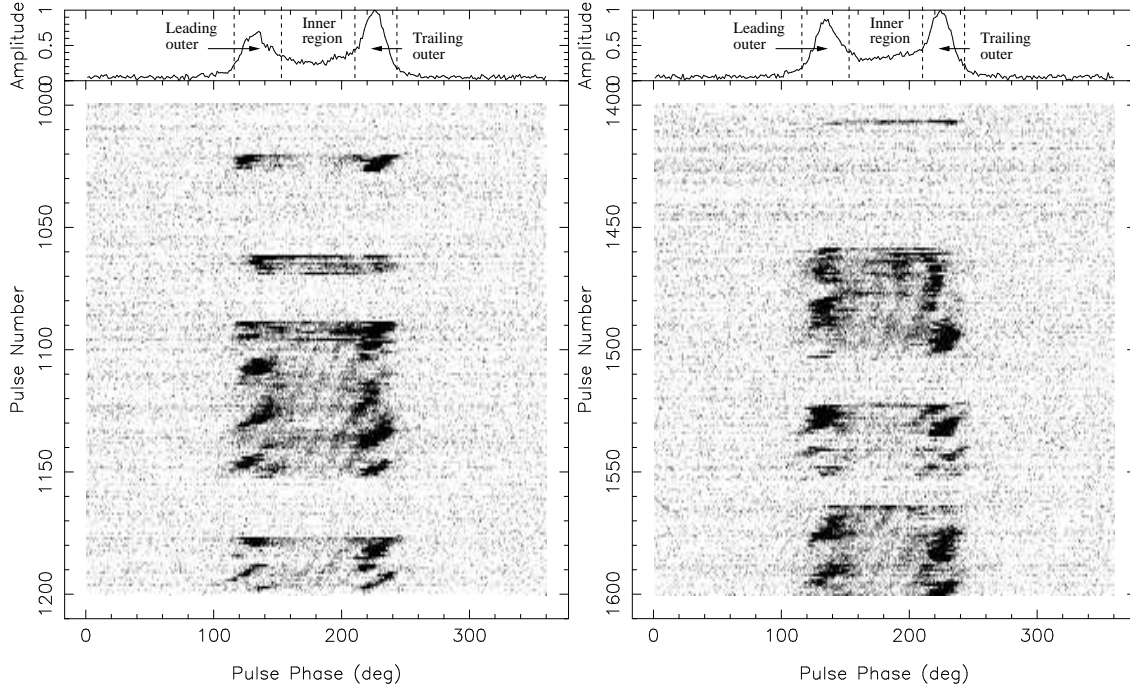


Figure 1. Gray scale plot of single pulses from PSR B0818–41 from observations on 24 February 2004 at 325 MHz. Left panel: pulse # 1000 to 1200; pulsar nulls from pulse # 1000 to 1020, pulse # 1028 to 1061, pulse # 1070 to 1088 and pulse # 1153 to 1176. Right panel: pulse # 1400 to 1600; pulsar nulls from pulse # 1409 to 1458, pulse # 1504 to 1521 and pulse # 1552 to 1563.

active pulse at the onset of the burst (after each null) appears to outshine the normal pulses. van Leeuwen et al. (2003) confirmed their results and also investigated the interaction between drifting and nulling in PSR B0809+74. They concluded that the drift pattern immediately after the nulls differs from the normal one and commented that, beside its normal and most common mode, the pulsar emits in a significantly different quasi-stable mode immediately after most, or possibly all, the nulls. In this mode the pulsar is brighter and the subpulse separation is less. They also reported that the subpulses drift more slowly and the pulse window is shifted towards the earlier longitudes. Investigating the interaction between drifting and nulling, Janssen & van Leeuwen (2004) determined the alias order for drifting of PSR B0818–13.

Though there has been significant progress both in the field of observations as well as understanding and characterising the phenomenon of nulling, the reason behind pulsar nulling and its connection to the emission mechanism is not tightly pinned down. In this regard, study of the emission properties before and after nulls, for individual pulsars, assumes importance. Remarkable subpulse drift pattern and frequent nulling is observed in PSR B0818–41 (Bhattacharyya et al. 2007). We find simultaneous occurrence of three drift regions with two different drift rates: an inner region with steeper apparent drift rate, flanked on each side by a region of slower apparent drift rate. The closely spaced drift bands always maintain a constant phase relationship: the subpulse emission from the inner drift region is in phase with that from the outer drift region on the right hand side, and at the same time the emission in the inner drift region is out of phase with the outer drift region situated on the left hand side. This phase locked relationship is maintained for the entire stretch of the data (for all the epochs of observations at 325 and 610 MHz) and does not appear to get perturbed after intermittent nulling or during changes in the drift rates. Although an extensive study of subpulse drifting and polarization properties of

this pulsar is presented in Bhattacharyya, Gupta & Gil (2009), its nulling properties remain hitherto unexplored. This paper reports a detailed investigation of the behaviour of this pulsar around nulls, from observations at 325 and 610 MHz. Results from our study are presented in Sect. 2. In Sect. 3 we discuss about the implications of the results and explain these with Partially Screened Gap model (Gil, Melikidze & Geppert 2003). Finally in Sect. 4 we summarise our findings.

2 ANALYSIS AND RESULTS

For the investigation of nulling behavior of PSR B0818–41, we have used single pulse observations at 325 MHz for two epochs (24 February 2004 and 21 December 2005, containing 3414 and 6600 pulses respectively) and at 610 MHz for two epochs (25 February 2004 and 11 January 2005, containing 1612 and 3600 pulses respectively). Details of the observations are described in Table 1 of Bhattacharyya, Gupta & Gil (2009).

We observe frequent nulling for PSR B0818–41. Duration of the nulls varies from few tens of pulses to a maximum of about a few hundred pulses. Fig. 1 shows a sample of the single pulse gray scale plots of PSR B0818–41 with both drifting and nulling at 325 MHz, from the GMRT observations on 24 February 2004. Fig. 2 plots the same, but from observations on 25 February 2004 at 610 MHz. Instances of pulsar in the null state are mentioned in the captions. Investigating the single pulse gray scale plots, we observe that the first active pulses in the bursts after the nulls look different from the normal pulses. For these pulses, the inner region appears more filled and is significantly more intense than that for the normal pulses (e.g. pulse #s 1062, 1089, 1177, 1459, 1522 and 1564 in Fig. 1). Though pulse # 1021, occurs just after a null and

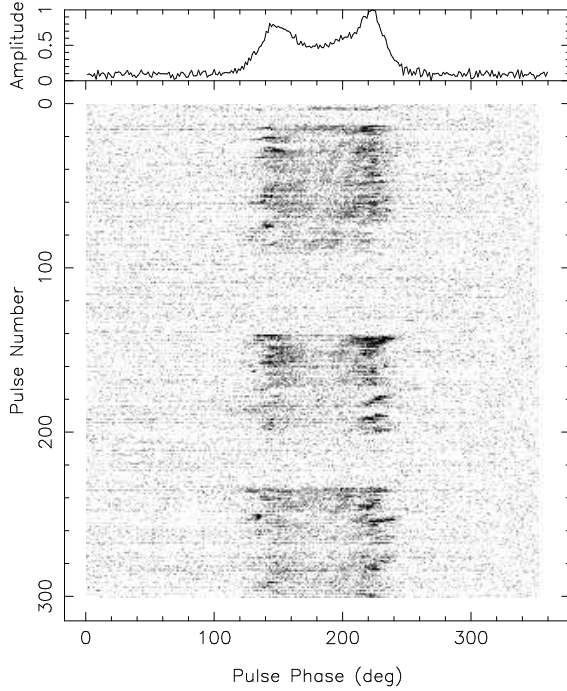


Figure 2. Same as Fig. 1, but for pulse # 1 to 300 from observations on 25 February 2004 at 610 MHz. Pulsar nulls from pulse # 3 to 13, pulse # 92 to 141 and pulse # 202 to 234.

does not greatly outshine the following pulses, it is brighter than the following pulses and is significantly brighter than the last active pulses before the null. Such cases with relatively less intense active pulses just after the nulls are rare, seen for $\sim 5\%$ of all the nulls, associated with shorter nulls (<10 pulses). On the other hand, the inner regions of the pulses just before the onset of the nulls (e.g. pulse #s 1027, 1152, 1503, 1551 in Fig. 1) appear less bright. In spite of being just before the onset of a null, pulse # 1069 is not less intense; this is also a rare exception seen typically for shorter nulls (<10 pulses), and consists $\sim 3\%$ of all the nulls. Association of changing drift rates with the nulls, which is discussed in details in Sect. 7.1 of Bhattacharyya, Gupta & Gil (2009), is quite evident in the single pulse gray scale plots.

2.1 Null distribution and identification of active and null pulses

Identification of the active and null states depends on the sensitivity limit of the telescope. High signal to noise (S/N) single pulse observations are required for accurate characterization of pulsar nulling properties. Ritchings (1976) and Biggs (1992) investigated the statistics of pulse energy distributions for characterizing the phenomenon of nulling. We follow a similar procedure for PSR B0818–41 and the corresponding ON pulse as well as OFF pulse energy histograms at 325 MHz from the observations on 24 February 2004, are shown in Fig. 3. At 325 MHz, the ON pulse histogram has two components corresponding to active and null pulses. We note (i) the strong presence of pulses with zero or near zero aggregate intensity, clearly indicating the occurrence of nulling and (ii) that the distribution is continuous between the pulses and the nulls, making it difficult to separate out the populations. At 610 MHz, the distributions tend to merge with each other as a consequence of lower S/N (Fig. 3). Using the method described in Ritchings

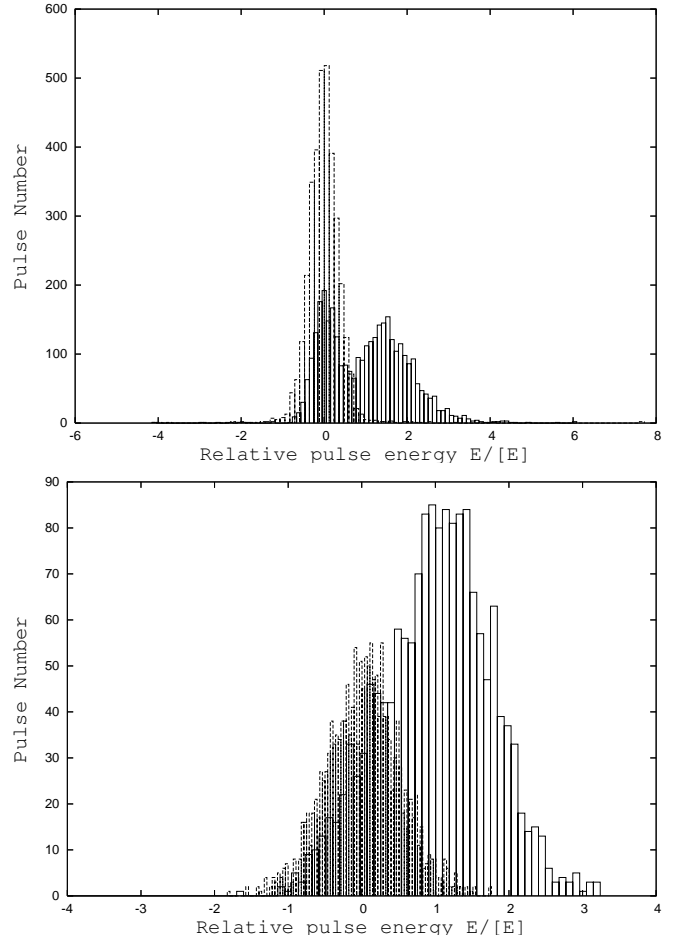


Figure 3. Energy histograms for PSR B0818–41. Those for the on pulse window are bars with solid lines; off pulse window are bars with dotted lines. Top panel: at 325 MHz with 3414 pulses, from observations on 24 February 2004. Bottom panel: at 610 MHz with 1612 pulses, from observations on 25 February 2004.

(1976), we calculate a nulling fraction of $\sim 30\%$ at 325 MHz, from the data of 24 February 2004, and a matching value of $\sim 28\%$ from the data of 21 December 2005. We can not estimate meaningful values from the 610 MHz data, as the ON and OFF distributions overlap significantly at this frequency, but the nulling fraction at 610 MHz seems to be consistent with the 325 MHz data.

Although pulse energy distributions provide statistical information about the nulling phenomenon, identifying individual nulls at each frequency is required for more detailed investigation. This is done by comparing the ON pulse energy estimate with a threshold based on the system noise level. The uncertainty in the pulse energy estimate $\sigma_{ep,on}$ is given by $\sqrt{n_{on}\sigma_{off}}$, where n_{on} is the number of ON pulse bins and σ_{off} is the rms of the OFF pulse region. Using this as a threshold, we classify pulses with ON pulse energy smaller than $3 \times \sigma_{ep,on}$, as null pulses. Using this, we are able to construct a ON/OFF time series of the single pulses, identify the lengths of the individual nulls and bursts, and also sequence the ON pulses just before a null and those in the burst just after each null.

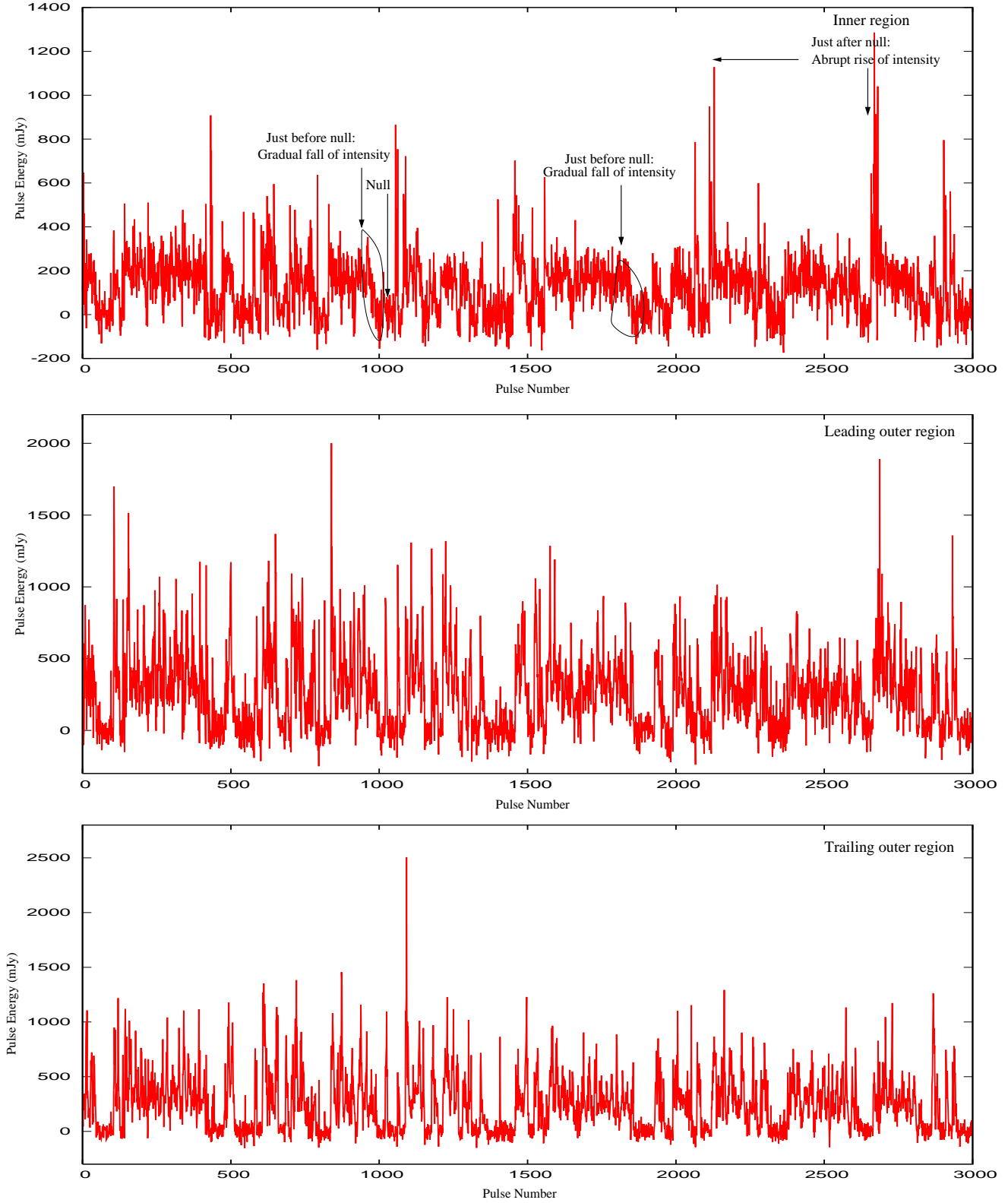


Figure 4. Top panel: Total energy of the inner region versus pulse number for the 3000 pulses of the 325 MHz data of 24 February 2004. Middle panel: Same as top panel, but for the leading outer region. Bottom panel: Same as top panel, but for the trailing outer region. Marked in the top panel are some instances of pulsar nulling, and the gradual decrease of intensity before the onset of the null, as well as examples of the sudden increase of intensity in the first few pulses when the pulsar turns on after the end of the null.

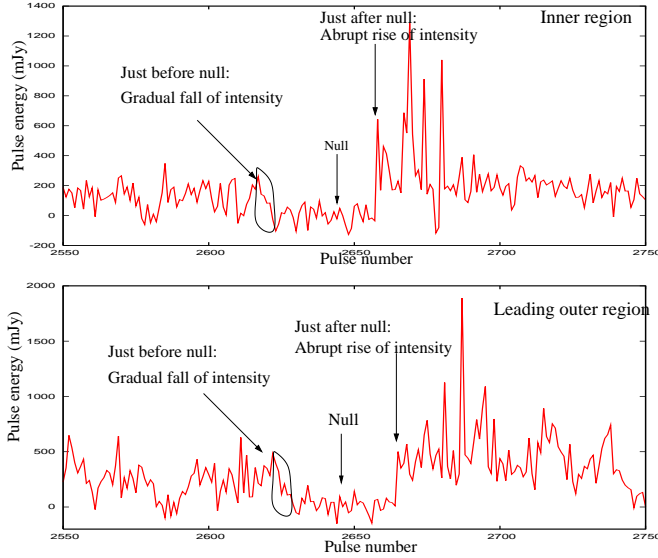


Figure 5. Top panel: Total energy of the inner region versus pulse number for a zoom in on pulse #s 2400 to 2800 from the 325 MHz observations on 24 February 2004. Bottom panel: Same as top panel, but for the leading outer region.

2.2 Durations of nulls and bursts

We aim to investigate any possible connection between the lengths of the bursts and the nulls. For example, does waiting longer for a null mean that it will last longer too? The durations of the nulls and the bursts immediately before and after the nulls are tabulated in columns 2,3 and 4 of Tables A1, A2, A3 and A4. We do not see any obvious correlation between the lengths of the nulls and the corresponding bursts, as well as between the null or burst lengths and the relative strengths of the pulses just before and after the nulls. Our result is similar to the study of PSR B0809+74 by van Leeuwen et al. (2003), who found that the lengths of the neighboring nulls and bursts are independent. This may indicate that there is no systematic dependence between the mechanism for nulling and the duration of nulls and bursts.

2.3 Pulse intensity variations before and after individual nulls

Fig. 4 plots the pulse energy versus the pulse number of the inner region as well as the leading and trailing outer regions of the pulse profile, for pulse # 1 to 3000 from observations on 24 February 2004 at 325 MHz (see Fig. 1 for definition of the inner and outer drift regions). The nulls are identified, in these plots, as the bunches of pulses of low energy, close to zero. An interesting trend can be seen, which is most prominent for the inner region (top panel of the figure) – the pulse intensity gradually goes down before the onset of a null, and suddenly shoots up for the first few active pulses in the burst. This trend is also present in leading and trailing outer regions, but is not as clear. A zoom in on one such typical event is shown in

Fig. 5, which plots the pulse energy for the inner and leading outer regions for pulse # 2550 to 2750. The gradual switching off before the null starts and the abrupt switching on at the beginning of the burst are clearly seen for both the emission regions, though with some differences in detailed properties, which are explored further in Sect. 2.4.

From these results we infer that the entire pulse energy appears to change in a fairly particular manner immediately before and after the nulls, though the variations are more clear for the inner region of the pulse. We believe this difference in behaviour may be due to the fact that the intensities of the leading and trailing outer regions of successive pulses are already significantly modulated at the 18.3 P_1 periodicity (referred to as P_3^m , see Bhattacharyya et al. (2007)), making it harder to detect the variations we are looking for. For the inner region, the averaging over the multiple drift bands helps to smooth out the P_3^m modulation effect. This is a reflection of the fact that in case of inner region our line of sight is grazing the emission ring, whereas for the leading and trailing outer regions we have a more central or direct traverse (see Fig. 7 and Fig. 8 of Bhattacharyya, Gupta & Gil (2009)).

Consequently, we choose the inner region for further quantitative investigation of these intensity modulations immediately before and after the nulls. We select the sequences of nulls for which pulsar is active for at least 10 pulses before the nulls, and the successive burst state lasts for at least 10 pulses. For the data at 325 MHz, where we are able to identify a total of 41 such sequences from the 10,000 pulse data at the two epochs, we find that the time taken for transition from the active to null state varies somewhat, with a minimum of about 5 pulse periods, maximum of about 13 periods, and a mean of about 10 periods. The transition from the null to the burst state is rather abrupt – the intensity rises to a maximum over a short time scale, less than one period, which is maintained for a few pulses before decaying down to the typical active state level. A similar trend is seen in the 17 events that are identified in the 5200 pulse data from the two epochs at 610 MHz.

For each event, we compute the following quantities for the inner region,

- $\langle I_b(1p : 10p) \rangle$: mean intensity of 10 active pulses immediately before the null.
- I_a : intensity of the first active pulse of the burst just after the null.
- $\langle I_a(4p : 10p) \rangle$: mean intensity of the 4th to 10th active pulses in the burst.¹
- $I_a / \langle I_b(1p : 10p) \rangle$: ratio of I_a to $\langle I_b(1p : 10p) \rangle$ which provides a comparison of the strength of the first active pulse of the burst to the mean strength of the last ten active pulses before the null.
- $I_a / \langle I_a(4p : 10p) \rangle$: ratio of I_a to $\langle I_a(4p : 10p) \rangle$ which provides a comparison of the strength of the first active pulse of the burst to the mean strength further in the burst.
- $\langle I_a(4p : 10p) \rangle / \langle I_b(1p : 10p) \rangle$: ratio of $\langle I_a(4p : 10p) \rangle$ to $\langle I_b(1p : 10p) \rangle$ which provides a comparison of the strength of the active pulses in the burst (from the fourth pulse onwards and up to the tenth pulse) to the mean of the last ten active pulses before the null.

The three ratios above are tabulated in Table 1 for the 325 MHz observations on 24 February 2004². We find that

¹ The first three active pulses are generally stronger than the rest. So we considered the mean intensity of fourth pulse onwards for comparison of intensities just at the onset of the burst to sufficiently after the onset.

² Same exercise tried with $\langle I_a(1p : 3p) \rangle$ or $\langle I_a(1p : 2p) \rangle$ in place of I_a produces similar ratios

Table 1. Investigation of the intensity distribution of the inner region immediately before and after the nulls (from observations at 325 MHz on 24 February 2004)

Serial Number	Duration of null	Duration of burst after null	Duration of burst before null	$\frac{I_a}{\langle I_b(1p:10p) \rangle}$	$\frac{\langle I_a(4p:10p) \rangle}{\langle I_b(1p:10p) \rangle}$	$\frac{I_a}{\langle I_a(4p:10p) \rangle}$
1	59	20	>46	1.89	0.86	2.19
2	5	276	21	3.12	1.94	1.61
3	50	33	282	1.73	0.62	2.81
4	92	52	39	2.11	1.73	1.21
5	25	10	54	1.78	1.46	1.21
6	49	83	83	2.93	1.87	1.57
7	27	10	35	1.85	0.61	3.01
8	33	10	10	5.97	3.43	3.12
9	18	64	10	1.28	1.12	1.15
10	23	21	64	1.83	0.71	2.55
11	14	52	21	2.07	1.52	1.35
12	12	31	52	1.02	0.69	1.46
13	28	17	31	1.49	0.85	1.76
14	17	31	40	1.67	0.99	1.69
15	11	294	31	5.56	1.89	2.95
16	17	14	64	5.52	2.70	2.04
17	34	150	14	3.07	1.47	2.09
18	8	28	150	6.99	2.36	2.97
19	62	207	28	1.43	0.62	2.28
20	10	35	207	2.11	0.91	2.32
21	37	148	35	5.20	3.01	1.73
22	10	11	10	1.75	0.87	2.02
Mean value	—	—	—	2.84	1.46	2.05
Median Value	—	—	—	1.98	1.29	2.03

Table 2. Same as Table 1, but from another epoch at 325 MHz on 21 December 2005

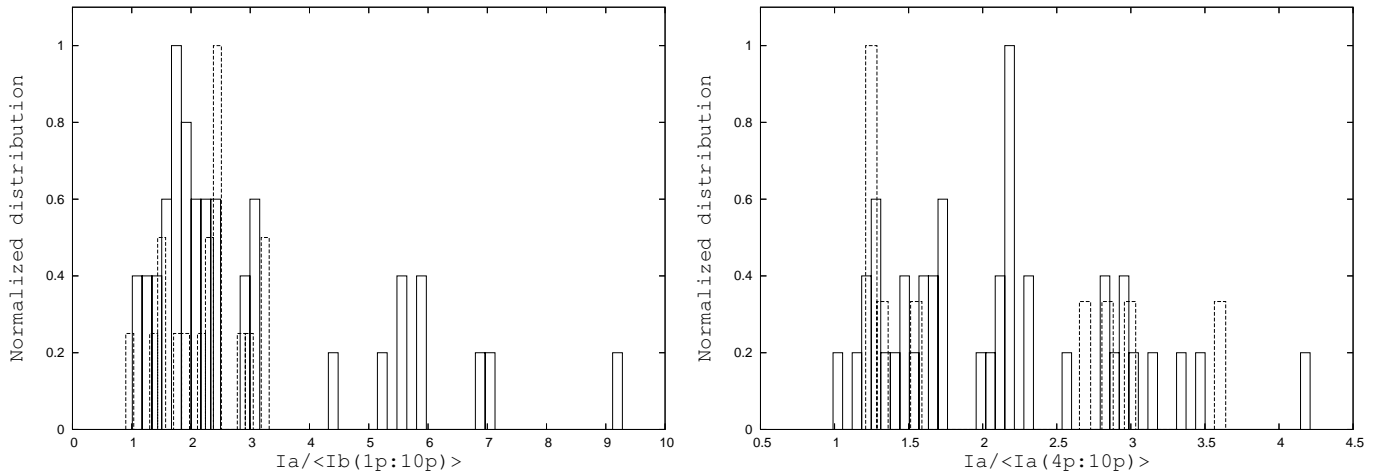
Serial Number	Duration of null	Duration of burst after null	Duration of burst before null	$\frac{I_a}{\langle I_b(1p:10p) \rangle}$	$\frac{\langle I_a(4p:10p) \rangle}{\langle I_b(1p:10p) \rangle}$	$\frac{I_a}{\langle I_a(4p:10p) \rangle}$
1	46	30	>46	2.25	1.67	1.53
2	83	203	474	5.95	2.10	2.84
3	28	202	185	2.18	1.02	2.15
4	10	250	202	2.25	1.31	1.71
5	268	145	103	6.83	1.96	3.48
6	86	150	145	9.28	2.20	4.21
7	22	51	150	2.91	1.38	2.11
8	10	125	56	2.39	1.83	1.31
9	104	47	120	1.84	0.55	3.35
10	48	49	274	2.34	0.80	2.90
11	23	17	49	2.38	1.08	2.20
12	50	105	17	1.87	1.24	1.50
13	41	15	370	1.82	1.84	0.99
14	330	109	15	1.01	0.71	1.42
15	8	50	109	1.26	0.96	1.30
16	159	184	50	3.06	2.33	1.31
17	23	22	184	1.56	0.93	1.67
18	103	33	199	4.39	2.02	2.18
19	22	73	30	1.67	0.76	2.19
Mean value	—	—	—	3.03	1.40	2.12
Median value	—	—	—	2.33	1.31	2.11

Table 3. Same as Table 1, but at 610 MHz on 25 February 2004

Serial Number	Duration of null	Duration of burst after null	Duration of burst before null	$\frac{I_a}{\langle I_b(1p:10p) \rangle}$	$\frac{\langle I_a(4p:10p) \rangle}{\langle I_b(1p:10p) \rangle}$	$\frac{I_a}{\langle I_a(4p:10p) \rangle}$
1	8	81	>5	1.88	0.52	3.64
2	47	61	81	2.15	0.76	2.85
3	32	793	61	3.32	2.59	1.28
4	98	24	793	3.19	1.19	2.66
5	33	78	24	1.53	0.97	1.58
6	28	15	78	2.44	0.81	3.02
7	19	48	15	1.51	1.25	1.21
8	37	47	48	2.29	1.73	1.33
9	18	115	47	2.26	1.81	1.24
Mean value	—	—	—	2.29	1.43	1.81
Median value	—	—	—	2.26	1.35	1.36

Table 4. Same as Table 1, but at 610 MHz on 11 January 2005

Serial Number	Duration of null	Duration of burst after null	Duration of burst before null	$\frac{I_a}{\langle I_b(1p:10p) \rangle}$	$\frac{\langle I_a(4p:10p) \rangle}{\langle I_b(1p:10p) \rangle}$	$\frac{I_a}{\langle I_a(4p:10p) \rangle}$
1	200	400	725	2.51	1.70	1.47
2	60	113	96	2.95	3.93	0.75
3	73	55	113	1.42	1.15	1.24
4	31	164	55	2.51	2.13	1.18
5	86	130	164	2.88	2.42	1.19
6	40	15	130	1.80	0.84	2.13
7	94	220	405	0.90	1.03	0.87
8	128	103	202	2.47	1.26	1.96
Mean value	—	—	—	2.18	1.81	1.35
Median value	—	—	—	2.49	1.48	1.21


Figure 6. Relative strength of the first active pulse in the burst to the pulses just before the onset of the null ($I_a/\langle I_b(1p:10p) \rangle$), shown in the left panel) and to the later pulses in the burst ($I_a/\langle I_a(4p:10p) \rangle$), shown in the right panel), from the ratios listed in Table 1, 2, 3 and 4. The solid and dashed lines denote the corresponding 325 and 610 MHz values.

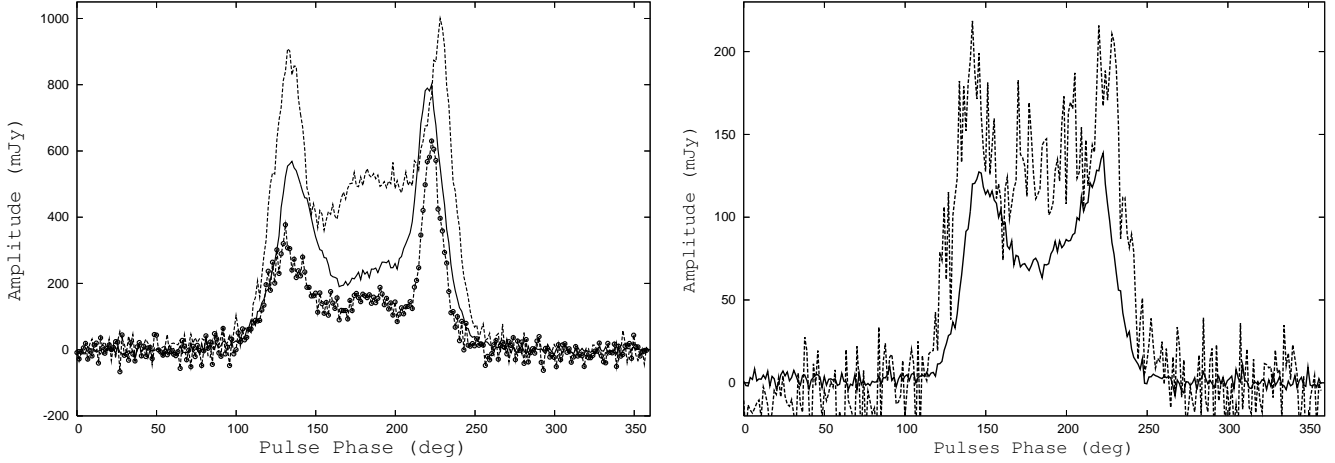


Figure 7. Left panel: The average profiles for regular drifting mode (solid line), first active pulse of the bursts (dashed line), last active pulses before the nulls (dashed line with open circles), at 325 MHz from the data of 24 February 2004 and 21 December 2005. Right panel: Normal average profile (dashed line) and the average profile from the first active pulse of the bursts (solid line) at 610 MHz from the data of 25 February 2004 and 11 January 2005.

$I_a/\langle I_b(1p : 10p) \rangle$ is always greater than unity with a mean of 2.8, confirming that first active pulse in the burst outshines the pulses just before the nulls. $\langle I_a(4p : 10p) \rangle / \langle I_b(1p : 10p) \rangle$ is comparatively less and oscillates around unity, with the mean over all the events coming to 1.5. $I_a/\langle I_a(4p : 10p) \rangle$ is always greater than unity (mean value ~ 2.0) signifying that the first few active pulses in the burst are brighter than those later in the burst. Table 2 lists the same as Table 1, but for observations at 325 MHz on the second epoch – the results are found to be very similar for both the epochs. Tables 3 and 4 give the corresponding results for 610 MHz, from data of 25 February 2004 and 11 January 2005. $I_a/\langle I_b(1p : 10p) \rangle$ is almost always more than unity with a mean around 2.2 at each epoch, which is a bit lower than the values at 325 MHz. Same is true for the comparison of $I_a/\langle I_a(4p : 10p) \rangle$ values between 325 and 610 MHz. However, the mean value of $\langle I_a(4p : 10p) \rangle / \langle I_b(1p : 10p) \rangle$ at 610 MHz is comparable or greater than the mean values at 325 MHz. The mean of $I_a/\langle I_b(1p : 10p) \rangle$ for all the null occurrences for both the frequencies is 2.8 and median is 2.3. Whereas the mean value of $I_a/\langle I_a(4p : 10p) \rangle$ for all the null occurrences for both the frequencies is 2.0 and median is 1.9.

Left panel of Fig. 6 is the plot of normalized distributions of $I_a/\langle I_b(1p : 10p) \rangle$ for all the epochs at 325 and 610 MHz. Right panel of Fig. 6 plots the same for $I_a/\langle I_a(4p : 10p) \rangle$. The implications of the above findings are discussed in Sect. 3.

From the above analysis we conclude that, at 325 MHz, the first few active pulses in the burst following a null are almost 3 times brighter than the last few pulses before the onset of the null (this ratio decreases to about 2.2 at 610 MHz); also these pulses are about 2 times brighter than the successive pulse in the burst state (this ratio is again lower at 610 MHz).

2.4 Average profile variations from pulses before and after nulls

The analysis presented in the previous section brings out the fact that the individual pulses immediately before and after the nulls have different characteristics than the normal pulses. To study the mean behaviour, we construct the average profiles of the pulses immediately before and after the nulls, for the nulls that satisfy the criterion described in Sect. 2.3. The left panel of Fig. 7 presents average pulse profiles of PSR B0818–41 at 325 MHz from the data

of 24 February 2004 and 21 December 2005 at 325 MHz from, (a) a sequence of 200 pulses showing regular drifting (hereafter referred to as normal profile) – solid line, (b) the last active pulse before the nulls – dashed line with open circles, and (c) from the first active pulse of the bursts – dashed line. We can see clearly that the average profile from the last active pulse before the nulls is significantly weaker than the normal profile, for both the leading and trailing outer regions, as well as for the inner region. It is also much weaker than the average profile from the first active pulse in the bursts, which has a significant bump of enhanced energy for the inner region, and comparable strengths for the leading and trailing outer regions, quite unlike the other two profiles. A similar behaviour is seen at 610 MHz. The right panel of Fig. 7 presents the average pulse profiles of PSR B0818–41 at 610 MHz from the data of 25 February 2004 and 11 January 2005, (a) a sequence of 300 pulses showing regular drifting (the normal average profile) – solid line, and (b) average profile from the first active pulse of the bursts – dashed line. The shapes of the profiles are somewhat similar, except for the bump of enhanced power in the inner region, which is also seen at 325 MHz. These results from average profiles at 325 and 610 MHz directly support the conclusions obtained from the study of individual nulling events in Sect. 2.3. It appears that the pulsar emerges from the nulls very much brighter in overall intensity, with a very specific change in pulse shape and energy distribution, which appears to be somewhat similar at the two frequencies.

We notice that these properties are pretty much the same for the two different epochs of 325 MHz data (e.g. Fig. 8), suggesting consistency in the observed properties of this pulsar before and after the nulls. To investigate this further, we have compared the average profiles at 325 MHz from the two epochs, for successive pulses in the bursts and also for successive pulses before the onset of nulls. The results are shown in Figs. 9 and Fig. 10. A noticeable similarity is observed between the corresponding average profiles from the two epochs, for the pulses in the burst, whereas the similarity is much less for the pulses before the onset of the nulls. This further supports the claim that the pulsar shows very characteristic changes in profile intensity, shape and energy distribution when it emerges from nulls. These changes are investigated further in detail in the next section.

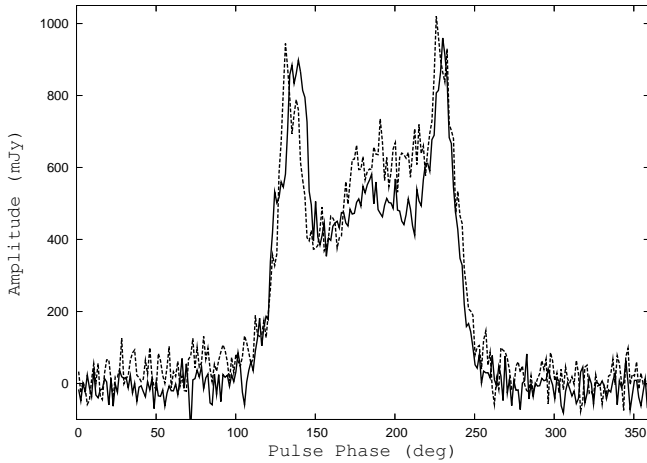


Figure 8. Comparison of the average profile from the first active pulse in the bursts from 325 MHz data of two epochs: 24 February 2004 (solid line) and 21 December 2005 (dashed line).

2.4.1 Variation of average pulse intensity around the nulls

In the following, we investigate in further detail the evolution of the intensity in different regions of the pulse profile, of the pulses around the nulls. Figs. 11 and 12 show the total intensity of the inner region and the leading and trailing outer regions, for the average profiles obtained from the addition of specific pulse numbers in the burst regions, as a function of the pulse number. In addition, Fig. 11 also shows the same for pulses before the onset of the nulls, for the inner region only. For the inner region, during the bursts, the mean intensity follows a clear, systematic trend: it is maximum for the first active pulse in the bursts (~ 520 mJy for the first epoch and ~ 650 mJy for the second epoch), and then gradually goes down. The intensity of the inner region reaches the value observed for the normal profile (~ 220 mJy for the first epoch and ~ 260 mJy for the second epoch) after about 20 active pulses in the burst³. It is notable that these variations of intensity with pulse number is strikingly similar for the two epochs.

The corresponding behaviour for the pulses before the onset of the nulls is somewhat less clear. The mean intensity of the inner region is less for the average profiles from these pulses (around 164 mJy for the first epoch and 187 mJy for the second epoch), and also shows some signature of a gradual decrease from the 20th to the last pulse before the onset of nulls (left panel of Fig. 11) – the value for the 20th pulse (214 mJy and 224 mJy for the first and second epochs, respectively) is quite close to the normal profile value. However, this behaviour is not as clear and systematic as that for the pulses in the bursts. One possible reason for this could be that as the decrease of intensity before the nulls happens over slightly different timescales for each individual null, the averaging process tends to blur out the trend. That this does not happen for the pulses in the bursts indicates that the behaviour of the pulsar as it emerges from the nulls is probably highly repeatable. It is thus likely that the pulsar magnetosphere reaches a very similar condition during the nulls and the pulsar turns on in a well defined, repeatable state after each null.

³ Peak to peak fluctuation of the mean off pulse intensity is used as the measure of error. Corresponding error bars denote 3-sigma errors.

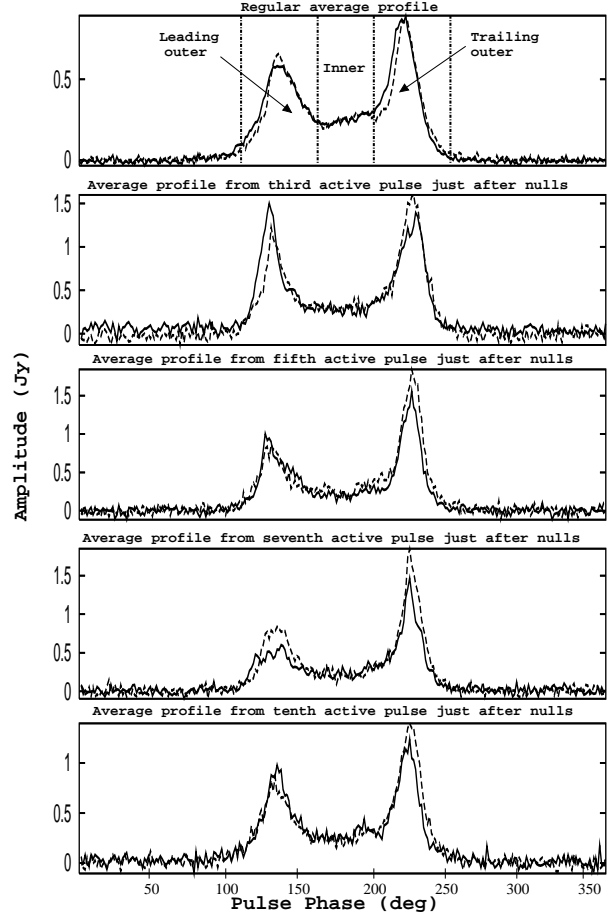


Figure 9. Comparison of the average profile from the third, fifth, seventh and tenth pulse in the bursts, for the two epochs at 325 MHz: 24 February 2004 (solid line) and 21 December 2005 (dashed line). The top panel shows the regular average profile, for comparison.

The variation of mean intensity for the leading and trailing outer regions of the profile (Fig. 12) is somewhat different from that of the inner region, for the pulses in the bursts. Though the intensity at the beginning of the bursts is higher, the peak is slightly delayed – it occurs at the second or third active pulse in the bursts for the leading component, and at the third or fourth pulse for the trailing component, rather than at the first pulse (as for the inner region). This delay can also be seen in Fig. 5 with careful observation. We would like to emphasize that the start and end of the nulls are defined by the inner region. The fall-off also appears to be somewhat more gradual than the 3-4 pulse decay seen for the inner region. The relative intensities of the leading and trailing outer regions also show a well defined behaviour. For the first pulse in the bursts, the two regions are of similar intensity (Fig. 8), and then the ratio evolves with pulse number and reaches the final value of 0.6 seen for the normal profile.

2.4.2 Variation of profile width of pulses around the nulls

Fig. 7 gives an indication that the positions of the leading and the trailing peaks of the average profile from the first pulses in the bursts are shifted from the normal. To check if there is a systematic behaviour of this with pulse number in the bursts, we take two

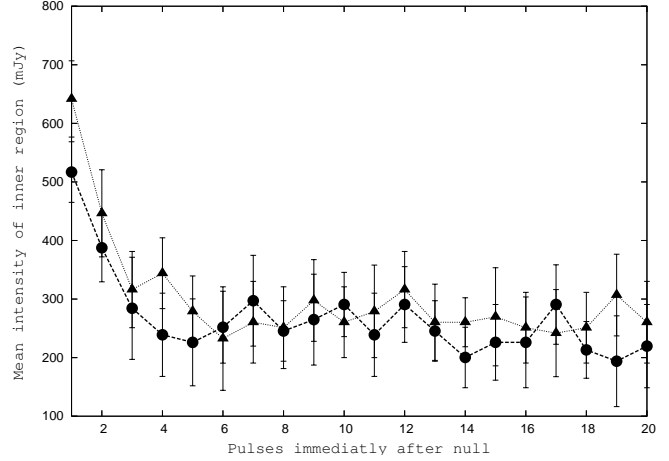
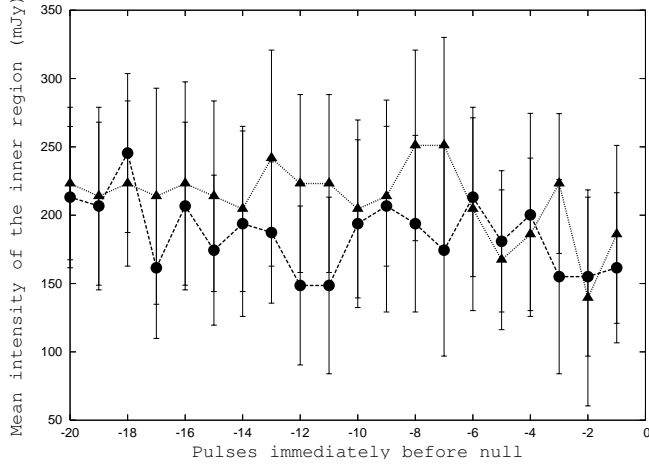


Figure 11. Left panel: Mean intensity of inner region of the average profile from the pulses immediately before the nulls versus the corresponding pulse number at 325 MHz. Right panel: Mean intensity of inner region of the average profile from the pulses immediately after the nulls versus the corresponding pulse number at 325 MHz. Results for the epoch on 24 February 2004 are denoted by dashed line and for the epoch on 21 December 2005 are denoted by dotted line.

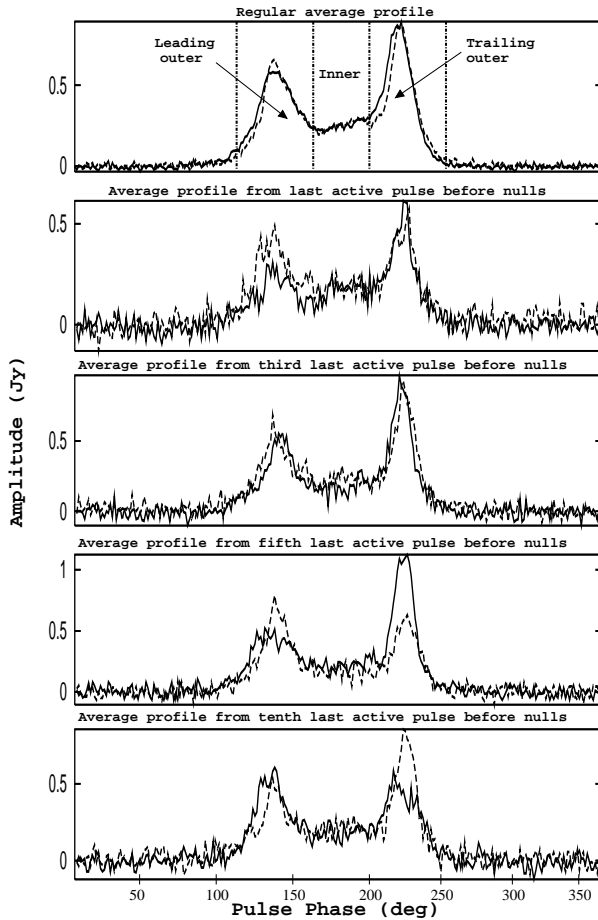


Figure 10. Comparison of the average profile from the first, third, fifth and tenth from last pulse before the onset of nulls, for the two epochs at 325 MHz: 24 February 2004 (solid line) and 21 December 2005 (dashed line). The top panel shows the regular average profile, for comparison.

consecutive active pulses in the bursts and calculate the mean average profile for these (e.g. average profiles from the first and second pulses, third and fourth pulses etc.). The positions of the leading and the trailing peaks are calculated for each of these mean profiles by fitting second order polynomials to the peaks. We combine two consecutive pulses, in order to increase the signal to noise of the resultant profile, which helps us fit a function to determine the position of the peak. Fig. 13 shows the positions of the fitted peaks for the leading and trailing sections as well as the separation between them, as a function of pulse number. The leading peak is shifted to earlier pulse phase (by about 3 to 4 degrees) at the beginning of the burst and slowly comes back to the normal profile position in about 10 pulses. The trailing peak is shifted to later pulse phase by somewhat larger amounts (about 6 degrees) at the beginning of the burst, and it also comes back to the normal profile position in about 10 pulses. As a result, at the beginning of the burst, the profile width, as defined by the separation between these two peaks, is larger by about 9 to 10 degrees from its normal value of 87 degrees, and relaxes to this normal value in about 8 to 10 pulses. Also, the center of the profile, defined by the point mid-way between the two peaks, is displaced to later pulse phase at the beginning of the burst (by about 2 degrees).

The above findings, which are very similar for both the epochs of observations, provide further evidence for a well defined change in the emission properties of the pulsar when it emerges from the nulls, and a systematic evolution of the same during the first few pulses of the bursts following the nulls.

2.5 Behaviour of drift pattern around the nulls

In Bhattacharyya, Gupta & Gil (2009), we have described the general behaviour of the drift pattern around the nulls for this pulsar. There is clear evidence for changes in the apparent drift rate just before and after the nulls. On several occasions, the apparent drift rate becomes less, i.e. drifting becomes apparently slower, often transitioning to an almost phase stationary drift pattern just before the onset of the null (see left panel of Fig. 14 for a typical example). A detailed examination of the nulls selected in Sect. 2.3 shows that this kind of behaviour is seen for $\sim 60\%$ of the occasions. For

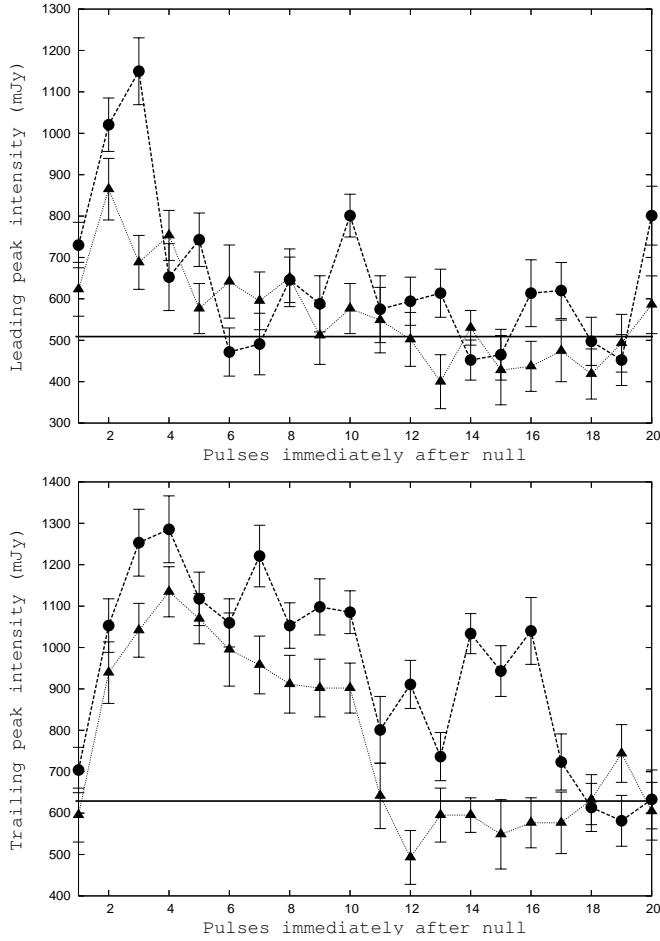


Figure 12. Top panel: Mean intensity of the leading peak of the average profile from the pulses immediately after the nulls versus the corresponding pulse number at 325 MHz. Bottom panel: same as the top panel, but for the trailing peak of the average profile from the pulses immediately after the nulls. For both cases, 5 bins on each side of the peak have been included, covering a pulse longitude range of 13.5 degrees. In both panels, results from the data of 24 February 2004 are shown by dashed lines and that of 21 December 2005 are shown by dotted lines; the horizontal solid lines indicate the corresponding values for the normal profile.

the remaining cases, there does not appear to be any appreciable change in the apparent drift rate.

The behaviour of the drift pattern just when the pulsar comes out of the nulls is also interesting. It often shows irregular drifting for a few pulses and then settles down to the normal drifting pattern (see right panel of Fig. 14 for a typical example). This kind of transition is seen after most of the nulls. It is likely that there is some connection between the intensity changes that the pulsar undergoes just before and after the nulls and the changes in the drift pattern seen at those times.

3 DISCUSSION

In the following we discuss about the implications of the new results from our study of the nulling properties of PSR B0818–41, and compare these with results reported in the literature for other pulsars. We also investigate the relevance of the Partially Screened Gap model in understanding some of our results.

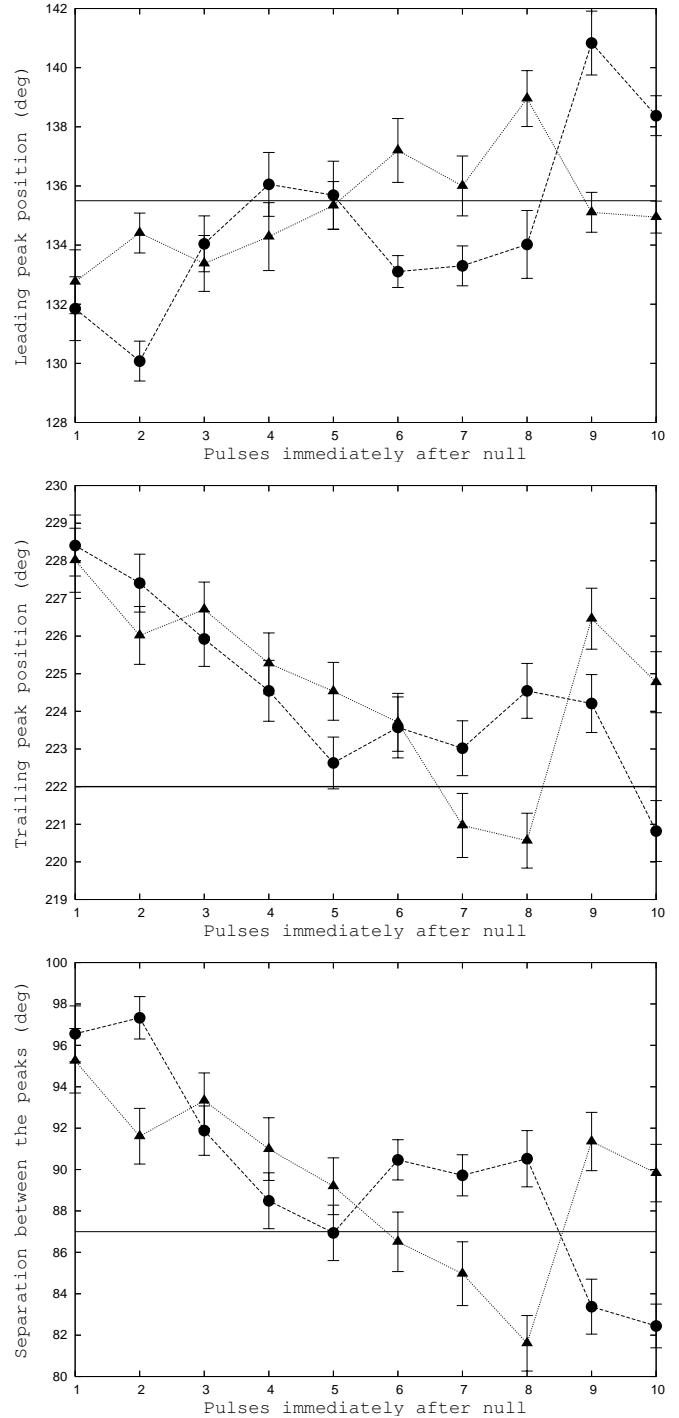


Figure 13. Top panel: Position of the leading peak of the average profile from the pulses at the beginning of the burst, versus the corresponding pulse number at 325 MHz. Middle panel: Position of the trailing peak of the average profile from the pulses at the beginning of the burst, versus the corresponding pulse number at 325 MHz. Bottom panel: Separation between these leading and trailing peaks versus the corresponding pulse number at 325 MHz. In each panel, results from the data of 24 February 2004 are shown by dashed lines and that of 21 December 2005 are shown by dotted lines; the horizontal solid lines indicate the corresponding values for the normal profile.

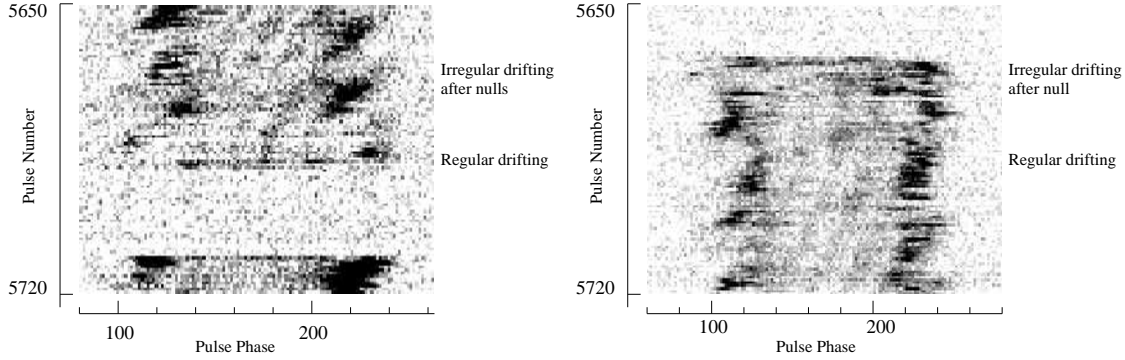


Figure 14. Gray scale plot of 70 single pulses of PSR B0818-41 at 325 MHz. Left panel: demonstrate the nature of drifting just before the nulls. Right panel: demonstrate the nature of drifting just after the nulls.

3.1 Intensity modulation around the nulls

Our investigations reveal a clear difference in the nature of the transitions from bursts to nulls to that from nulls to bursts. The pulsar's radio energy appears to reduce gradually for a few pulses before it finally switches off at a null. The time scale of this fading ranges from about 5 to 13 pulses, for different nulls. On the other hand, the transitions from nulls to bursts are abrupt and furthermore, the pulsar's radio energy for the first few pulses in a burst is significantly larger than the average value. For the inner region, the brightening from just before the nulls to the beginning of the burst is, on an average, close to 3 times, at 325 MHz. This ratio appears to show some frequency dependence, dropping to close to 2 at 610 MHz. For the outer regions, the brightening is about 2 times at 325 MHz. In addition, the brightening of the outer regions happens with a delay of 2-4 pulses from the beginning of the burst, unlike the inner region where the first pulse in the burst is the brightest and the intensity decays monotonically after that.

It is interesting to check if other pulsars also show such a behaviour, or is PSR B0818-41 unique in this context. For PSR B0031-07, Vivekanand (1995) reported that both bursts and nulls are mostly quite abrupt, but in $\approx 20\%$ of cases the onset of nulling is slow, occurring over one to several periods. No significant relative brightening from before to after nulls (in an average sense) is reported by them for this pulsar. Fig. 4 of Rankin & Wright (2008) plots pulse energy versus pulse number for PSR J1819+1305, where we note a clear signature of gradual decrease in energy in the last active pulses before the onset of the nulls, and sharp transitions from nulls to bursts, with first pulses in the bursts being much brighter than the normal pulses. This is, however, not mentioned and discussed by the authors in the paper. PSR B1944+17 is another pulsar for which the transitions from nulls to bursts are known to be quite different in character from the transitions from bursts to nulls. Deich et al. (1986) reported that the switching off of this pulsar is preceded by a slow (~ 3 pulses) decay in average intensity. They also find a higher relative brightness of the first active pulse in the bursts, compared to the average strength. For PSR B0809+74 also, Lyne & Ashworth (1983) find that the last active pulse before nulls is dimmer than the normal pulses, and the first active pulse in the bursts is brighter than normal.

Thus, it appears that there is some evidence in the general pulsar population for the kind of behaviour that we report for PSR B0818-41. For some nulling pulsars, such systematic intensity modulations may be partially masked by modulations due to other causes such as drifting subpulses, as we find for the outer regions of PSR B0818-41. For the inner region, where the grazing line

of sight samples a larger portion of the emission region, subpulses from multiple drift bands are averaged and as a result, intensity modulations due to these are smoothed out. This warrants a more detailed study of the intensity modulations around nulls for other pulsars.

3.2 Shape and width of pulses around the nulls

We have reported significant evolution of the shapes of the pulses around the nulls, especially at the beginning of the bursts. Shape changes of the first few pulses in the bursts include the enhanced bump of intensity in the inner region, a more symmetric profile with the ratio of strengths of the leading and trailing components becoming close to unity. This is accompanied by an increase of about 10% in the width of the profile, as well as a shift of the mid-point towards the trailing side.

Such effects are seen in some other pulsars also. Janssen & van Leeuwen (2004) reported significantly different shapes of the average profiles from pulses before and after the nulls for PSR B0818-13 – the average profile from the last and first active pulses immediately before and after the nulls are observed to be double peaked, whereas the normal average profile are observed to be single peaked. For PSR B1944+17, Deich et al. (1986) reported that the last pulse before null has a shape that is quantitatively different and more variable than the shapes of other pulses. For PSR B0809+74, (van Leeuwen et al. 2003) found that though the pulses immediately before and after the nulls are similar in shape to the average profile, the peak of average profile from the first active pulse in the bursts after nulls is shifted towards earlier pulse longitude. As an explanation for this, van Leeuwen et al. (2003) proposed that after the nulls sub-beam carousel is smaller, indicating that we are looking deeper in the pulsar magnetosphere than we do normally. Finally, as an exception, we mention the case of PSR B0031-07, for which Vivekanand (1995) did not find any significant difference in the average profiles from the first active pulse in bursts, the last active pulse before the nulls, and the normal average profile.

For PSR B0818-41, the change in pulse width and center of the profile that is reported by us can be interpreted as a change in the distribution of the emission regions in the pulsar's magnetosphere. The pulse width can increase if either the cone of emission originates from a higher altitude on the same set of field lines, or if it shifts to outer field lines while maintaining a constant altitude. A combination of both these effects is also possible. If a increase in height alone was responsible, then the mid-point should have

moved to earlier longitudes, due to increased aberration and retardation effects (Gangadhara & Gupta 2001). If a change of field line alone was responsible, then the mid-point should have remained at the same longitude. The observed behaviour appears to require a combination of a shift to more outer field lines along with a reduction in the emission height. The shift to an outer set of field lines needs to be such that it produces an increase in the pulse width which is somewhat larger than observed. Some of this increase would then be compensated by the reduced height of emission, which should also be enough to produce the observed shift of the mid-point to later longitudes.

3.3 Drift rate around the nulls

The above picture becomes even more interesting when we add the information about the changing drift rates just before and after the nulls. It appears that as the pulsar's radio intensity dims gradually before the nulls, there is often an accompanying reduction in the drift rate. Further, when the pulsar comes out of the nulls, the increased radio intensity for the first few pulses is very often accompanied by what looks like a disturbed drift rate behaviour, which settles down to the regular drift pattern as the pulsar intensity returns to normal. This correspondence of intensity behaviour with drift rate variations, though not indisputably strong, is nevertheless quite striking and suggests a common cause. One such possibility is explored in the next section.

What is known about this kind of property for other pulsars? Investigating drifting around the null for PSR B0809+74, van Leeuwen et al. (2003), found that drift rate just before a null does not deviate from the normal drift rate. However, drift rate just after nulls is different from the normal drift rate. After the nulls PSR B0809+74 goes to a quasi-stable mode. They also found that drift rates after longer nulls are lower than the normal average drift rate.

From the discussions in Sect. 3.1, 3.2 and 3.3, it is clear that there are some very specific and well correlated changes that are seen in the radio emission properties of PSR B0818–41 when it restarts emission after a null. The fact that these changes are seen to be quite similar on two different epochs of observations strongly supports that these are stable, intrinsic changes and are tightly coupled to the nulling process. This points strongly to a scenario where the electromagnetic conditions in the region of the magnetosphere responsible for the radio emission reach a well defined “state” during or towards the end of each null; in other words, some kind of a “reset” of the pulsar's radio emission engine takes place, as a result of which the pulsar starts with a very characteristic post-null behaviour that slowly evolves towards a different kind of behaviour which characterises the average properties of the pulsar. Just before the onset of null, though the behaviour is fairly characteristic, it is not as stable or repeatable as that just after the nulls. In the following we explain some of these results with Partially Screened Gap model.

3.4 Explanation with the Partially Screened Gap model

According to the widely accepted picture, each radio subpulse can be associated with a radio sub beam passing through our line of sight, which is emitted at some altitude (canonically about 50–100 stellar radii) within a plasma column that is directly related to a spark discharge within the inner acceleration region near the polar

cap surface. The spark discharge produces a Goldreich Julian density of the primary (highly relativistic) column of plasma, which is then Sturrock multiplied and formed into a column of very dense but much less relativistic secondary plasma. Complicated non-linear processes in these plasma lead to the generation of the coherent radio emission associated with the observed subpulse (e.g. Cheng & Ruderman (1980), Filippenko & Radhakrishnan (1982), Melikidze, Gil, & Pataraya (2000), Mitra & Gil (2009)). There is no clear picture about how the energy density is propagating from the spark to the unstable secondary plasma and then to the radio emission beam. However, one can assume that the stronger the electric field in the acceleration region the stronger is the radio intensity of the observed subpulses. The prototype of the inner acceleration region was the pure vacuum gap model of Ruderman & Sutherland (1975). It is now understood that this model predicts too fast a subpulse drift since the electric field in pure vacuum gap is too strong. Much better agreement with the observational data of drifting subpulses is achieved within the so-called Partially Screened Gap model (hereafter PSG) (Gil, Melikidze & Geppert (2003), Gil et al. (2008)), in which the electric field is screened and lowered by factor of about 10 due to thermal emission of iron ions from the hot polar cap surface. The polar cap is heated due to the reverse flow of electrons from the magnetically created electron-positron pairs, even as the accelerated positrons leave the acceleration region. The heating produces thermal ejection of ions from the surface, which partially screens the gap electric field. The PSG model postulates that the polar cap temperature, T_s , reaches a quasi-equilibrium value, slightly below the critical ion temperature, T_i . This quasi-equilibrium is established by a subtle thermostatic balance between the heating due to back-flow bombardment and cooling due to radiation: the higher the T_s , the larger the thermo-emission of positive ions, which screens the potential drop in the gap, reduces the acceleration of the charges, thereby reducing the heating effect and thus leads to a decrease in the temperature (see Gil, Melikidze & Geppert (2003) for details). In the equilibrium condition, the value of T_s is about few percent lower than T_i (which is about 10^6 K), whereas the potential drop is only a few percent of the vacuum gap value (see Appendix in Gil et al. (2008)).

It is quite likely that the actual surface temperature T_s varies slightly around a thermostatically determined value on relatively slow time scales of longer than pulsar period. These tiny variations with an amplitude of few thousands K can be crucial for the pulse nulling phenomenon. We speculate that a null occurs when the polar cap temperature raises by few thousands K to a value at which the potential drop is screened to a level making generation of detectable radio emission impossible. In this phase the remnant potential drop can still drive enough pair production to heat the polar cap surface but not enough to generate detectable radio emission higher up in the magnetosphere. This residual heating is very important and its actual amount will determine the time of null duration. Without a residual heating the nulls would be extremely short (below 100 ns; Gil, Melikidze & Geppert (2003)) and unnoticeable. After some time the radiation cooling prevails and the temperature drops back few thousands K to the PSG thermostatic regime. The pulsar is back in the normal emission mode. Most likely, before reaching the quasi-stationary value the epoch of even lower temperatures will be reached, when the potential drop is even higher and the drift is fast, aliased and chaotic.

The electric field in the inner acceleration region above the polar cap results from deviations of the actual charge density from the co-rotational Goldreich-Julian (1969) value. This “non-co-rotational field” has two natural components: parallel and per-

pendicular to the surface magnetic field B . The parallel component causes acceleration, and in consequence pair plasma production which is utilized in the radio emission generation process further away. Also the heating of the polar cap surface, including thermal ions ejection, are due to this parallel component. Second component is tangent to the surface of the polar cap. This component causes the spark plasma circulation around the polar cap and in consequence subpulse drift across the pulse window. It is obvious that any variation of the gap electric field concerns both components. Therefore, the decrease/increase of the subpulse intensity should be correlated with slowing down/speeding up of the (non-aliased) subpulse drifting. In other words, the gradual decrease of subpulse intensity observed just before a null should be associated with the gradual slowdown of the subpulse drift. Exactly such a correlation is reported in our paper and its explanation (at least qualitative) seems clear. Just before a null the gap electric field decreases gradually on the time scales of several to few tens of pulsar periods, which causes a gradual drop of both the subpulse intensity and their drift rate. We speculate that this gradual decrease of gap electric field is caused by a small increase of the surface temperature which is estimated later in this section.

After the nulls the intensity rises to maximum over a short (less than one period) time scale, keeping a high intensity for a number of pulses (often randomly scattered over the pulse window). Then the normal drifting mode begins, with intensity slightly lower than those just after the nulls. This behaviour suggests strongly that at some point during a null the electric field begins to rise again and as soon as it reaches a critical value the PSG resumes an operation and the pulsar is back in action. Again, one can speculate that this rise of the electric field is associated with a small drop of the surface temperature. Right after the null the electric field is probably stronger than in the stable normal drifting mode. This is why the subpulses after a null are initially stronger than in the normal mode. We believe that under this strong electric field the spark circulation is very fast but also slowing down quickly as the electric field decreases. The system goes through fast variations of carousel circulation speed, which may result in the erratic behaviour of the observed subpulses. Later, after few to several pulses the PSG reaches the stable state and resumes normal operation. The pulsar is back in the normal drifting mode.

Using the phase offset between the leading and the trailing outer regions, we found that subpulse drifting in PSR B0818–41 is most likely first order aliased (Bhattacharyya, Gupta & Gil 2009). The carousel rotation period $P_4 \sim 18.3 P_1$ and time interval between recurrence of successive drift bands at a given pulse longitude $P_3^t = 0.95 P_1$. The observed slowing down of the drift rate to the point of phase stationary apparent drift bands just before the nulls (discussed in Sect. 2.5) means that P_3^t is close to P_1 . Hence, just before the nulls P_3^t must increase by about 5% (from 0.95 to about 1.0). This small variation of drift rate could be due to small change in the neutron star's surface temperature (Gil, Melikidze & Geppert 2003). In the following we estimate required change in polar cap temperature to increase P_3^t by 5%. Within the PSG model the actual potential drop is set at the level of few percent of the maximum possible Ruderman & Sutherland (1975) value, i.e. $\Delta V = \eta V_{RS}$, where the screening factor $\eta = 1 - \rho_i / \rho_{GJ} = 1 - \exp[C(1 - T_i/T_s)]$ and the coefficient C depends on the chemical composition of the surface layer (Medin & Lai (2007), Gil et al. (2008)). In the carousel scenario of the subpulse drift based on the PSG model $P_4 \sim \eta^{-1} r_p / h = NP_3^t$, where r_p is the polar cap radius, h is the height of the acceleration region and $N \sim 2\pi r_p / (2h) = \pi r_p / h$ is the number of sparks

circulating around the polar cap. Thus, the basic drifting periodicity $P_3^t = \eta^{-1} / \pi = 0.318 / \eta$. Assuming that ion critical temperature $T_i = 2 \times 10^6$ K (which seems to be a typical value; Gil et al. (2008)), for change of P_3^t from 0.95 to 1.0; the screening factor η must change from 0.335 to 0.318 and hence the corresponding ratios T_s/T_i , will be equal to 0.98658 and 0.9874, respectively. The required change in the surface temperature is $\Delta T_s = 0.00082 T_i = 1640$ K (from 1.973 to 1.9748 MK). So, to explain 5% slow-down of drift in B0818–41 just before the onset of the nulls, one would have to invoke about 0.1 % polar cap surface temperature variation. Based on the PSG model Gupta et al. (2004) argued (see their section 4.4) that only about 0.14 % change in the surface polar cap temperature (i.e. a change of about 4000 K around 2×10^6 K average temperature) is needed to cause this 8 % slow-down of drift signatures in B0826–34; which is of the same ballpark to our estimation for B0818–41.

Based on the frequency evolution of average profile, the observed PA swing and the analysis of subpulse drift signatures we proposed two possible geometries for this pulsar, **G-1** ($\alpha = 11^\circ$, $\beta = -5.4^\circ$), and **G-2** ($\alpha = 174.5^\circ$, $\beta = -6.9^\circ$) in Bhattacharyya, Gupta & Gil (2009). Pulsar radiation pattern simulated with both the geometries reproduces the observed features, except for some differences. Although **G-2** provides a reasonable fit to the overall PA curve at 325 MHz, and the left half of the PA curve at 610 MHz, only the middle part of the PA curve at 610 MHz can be fitted with **G-1**. On the other hand **G-1** appears to give better match on the observed P_2^m (longitude separation between the drift bands) values and the over all drift pattern. Both the geometries can explain the slight changes of apparent drift rates and phase stationary drift bands, once aliasing of drifting subpulses is considered. The observed slow down of apparent drift rate before nulling can be interpreted as slowing down of the carousel in **G-1** and speeding up of the carousel in **G-2** (see Sect. 7.1 of Bhattacharyya, Gupta & Gil (2009)). However, within the PSG model the accelerating gap electric field must increase to cause the speed up of the sparking carousel; and electric field should decrease to cause the slow-down of the same. A correlation between the gradual slowdown of the drift rate and gradual decrease of pulse energy is expected within the inner gap acceleration model. Hence, the fact that we do observe the gradual intensity decrease over a number of pulses just before the nulls strongly suggests that the accelerating electric field decreases in this stage of pulsar activity. This automatically implies that the carousel slows-down before the nulls, which is the case for **G-1**. Thus comparison of the prediction of PSG model with observations favors **G-1** over **G-2**.

4 SUMMARY

Following are the interesting new results from our investigation of the nulling properties of PSR B0818–41.

- The pulsar shows well defined nulls, lasting in duration from a few tens of pulses to a few hundreds of pulses; the estimated nulling fraction at 325 MHz is about 30%.
- The transitions from bursts to nulls are gradual (~ 10 pulse period on average), whereas the transitions from nulls to bursts are rather abrupt (less than one pulse period). The last few active pulses before the nulls are less intense than the normal, whereas the first few active pulses just after the nulls outshine the normal pulses. This effect is more evident for the inner region – the first few active pulses just after the nulls are about 2.8 times more intense than those before the nulls. Before the nulls, the

intensity decreases gradually over about 10 pulsar periods, during which generally the apparent drift rate slows down (often showing apparent longitude stationary drift bands just before the nulls). At the beginning of the bursts, the intensity rises to maximum in less than one period, keeping a high intensity for a number of pulses (often randomly scattered over the pulse window). Then the normal drifting mode begins, with intensity slightly lower than that just at the beginning of the burst.

- We observe significant evolution of the shapes of the pulses at the beginning of the bursts. Average profile from the first active pulses in the bursts has a significant bump of enhanced energy for the inner region, and comparable strengths for the leading and trailing outer regions, quite unlike the normal profile. The width of the average profile from the pulses just after the nulls is about 10% more than that of the normal. This is accompanied by a shift of the profile mid-point towards the trailing side. Some of these effects can be explained by a shift of the emission regions to different heights and/or somewhat outer field lines in the pulsar magnetosphere.

- We observe a very characteristic post-null behaviour of PSR B0818–41 when it restarts emission after a null. This indicates that some kind of “reset” of the pulsar’s radio emission engine takes place during the nulls, and immediately after the nulls the conditions of magnetosphere responsible for the radio emission are well defined.

The results presented in this paper indicates that phenomenon of nulling is intrinsic to the pulsar radio emission that is systematically ceased during the nulls. This study will put constraint on the models explaining pulsar radio emission and nulling. We successfully explained many of our results with the help of PSG model. However, some remains to be explained, for example, why nulling is associated with fast rise and slow fall of intensity, why intensity distribution across the profile immediately after the nulls is different than typical. More importantly, how the gap electric field varies around the nulls and what could actually cause a radio null, remains to be explained. Considering the PSG model, the actual mechanism of generation of the coherent radio emission must be very sensitive to tiny changes of the input parameters. We intend to devote a separate paper to this and the other problems mentioned above. Clearly, investigations of the pre and post null emission properties of PSR B0818–41, presented in this paper, emphasize that nulling provides a useful tool to probe the pulsar radio emission. Though, there is some evidence in general pulsar population for the kind of behaviour that we report for PSR B0818–41, for some pulsars such systematic modulations may be partially masked by modulations due to other causes such as drifting subpulses. This warrants a more detailed study of emission properties around the nulls for other pulsars.

Acknowledgments: We thank the staff of the GMRT for help with the observations. The GMRT is run by the National Centre for Radio Astrophysics of the Tata Institute of Fundamental Research. BB thanks Ramesh Bhat for his comments at very early stage of the work. We would like to thank our referee Patrick Weltevrede for his suggestions which had improved the paper. JG acknowledges a partial support of the Polish Research Grant N N203 2738 33.

REFERENCES

Biggs, J., D., 1992, *ApJ*, **394**, 574.

- Bhattacharyya, B., Gupta, Y., Gil, J., Sendyk, M., 2007, *MNRAS*, **377L**, 10.
- Bhattacharyya, B., Gupta, Y., Gil, J., 2009, *MNRAS*, **398**, 1435.
- Bhat, N. D. R., Gupta, Y., Kramer, M., Lyne, A. G., Johnston S., 2007, *A&A*, **462**, 257.
- Cheng, A. F., Ruderman, M. A., 1980, *ApJ*, **235**, 576.
- Deich, W. T. S., Cordes, J. M., Hankins, T. H., Rankin, J. M., 1986, *ApJ*, **300**, 540.
- Filippenko, A. V., Radhakrishnan, V., 1982, *ApJ*, **263**, 828.
- Gil, J., Melikidze G. I., Geppert U., 2003, *A&A*, **407**, 315.
- Gil, J., Haberl, F., Melikidze, G., Geppert, U., Zhang, B., Melikidze, G., Jr., 2008, *ApJ*, **686**, 497.
- Gupta, Y., Gil, J., Kijak, J., Sendyk, M., 2004, *A&A*, **426**, 229.
- Gupta, Y., Gangadhara, R. T., 2001, *ApJ*, **555**, 31.
- Herfindal, Jeffrey L., Rankin, J. M., 2007, *MNRAS*, **380**, 430.
- Janssen, G. H., van Leeuwen, J., 2004, *A&A*, **425**, 255.
- Lyne, A. G., Ashworth, M., 1983, *MNRAS*, **204**, 519.
- Medin, Z., Lai, D., 2007, *MNRAS*, **382**, 1833.
- Melikidze, G. I., Gil, J., Pataraya, A. D., 2000, *ApJ*, **544**, 1081.
- Mitra, D., Gil, J., Melikidze, G. I., 2009, *ApJL*, **696**, 141.
- Rankin, J. M., 1986, *ApJ*, **301**, 901.
- Rankin, J. M., Wright, G. A. E., 2008, *MNRAS*, **385**, 1923.
- Ruderman, M. A., Sutherland, P. G., 1975, *ApJ*, **196**, 51.
- Ritchings, R. T., 1976, *MNRAS*, **176**, 249.
- Vivekanand, M., 1995, *MNRAS*, **274**, 785.
- van Leeuwen, A. G. J., Stappers, B. W., Ramachandran, R., Rankin, J. M., 2003, *A&A*, **399**, 223.

